Molecular cloning and characterization of Brugia malayi thymidylate kinase

ARTICLE *in* ACTA TROPICA · FEBRUARY 2014

Impact Factor: 2.27 · DOI: 10.1016/j.actatropica.2014.02.003 · Source: PubMed

10 AUTHORS, INCLUDING:

Anita Verma
Central Drug Research Institute
10 PUBLICATIONS **11** CITATIONS
SEE PROFILE

Vikash Kumar
Central Drug Research Institute
24 PUBLICATIONS **104** CITATIONS
SEE PROFILE

Vishal M. Balaramnavar
Central Drug Research Institute
24 PUBLICATIONS **75** CITATIONS
SEE PROFILE

Jitendra Kumar
bharat sawak samaj channi
841 PUBLICATIONS **14,175** CITATIONS
SEE PROFILE

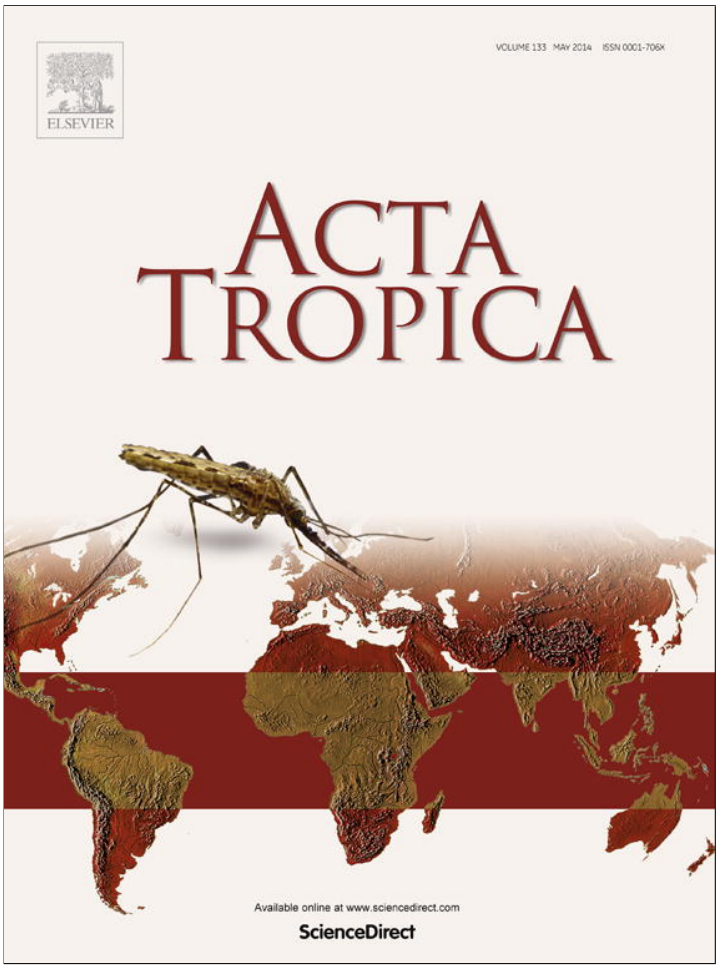

Acta Tropica 133 (2014) 83–92

Contents lists available at ScienceDirect

Acta Tropica

journal homepage: www.elsevier.com/locate/actatropica

Molecular cloning and characterization of *Brugia malayi* thymidylate kinase

Pawan Kumar Doharey[a], Manish Kumar Suthar[a], Anita Verma[a], Vikash Kumar[b], Sunita Yadav[a], Vishal M. Balaramnavar[c], Sushma Rathaur[d], Anil Kumar Saxena[c], Mohammad Imran Siddiqi[b], Jitendra Kumar Saxena[a,*]

[a] Division of Biochemistry, CSIR – Central Drug Research Institute, Lucknow 226001, Uttar Pradesh, India
[b] Division of Molecular and Structural Biology, CSIR – Central Drug Research Institute, Lucknow 226031, Uttar Pradesh, India
[c] Medicinal and Process Chemistry Division, CSIR – Central Drug Research Institute, Lucknow 226031, Uttar Pradesh, India
[d] Department of Biochemistry, Banaras Hindu University, Varanasi 221005, Uttar Pradesh, India

ARTICLE INFO

Article history:
Received 29 July 2013
Received in revised form 3 February 2014
Accepted 7 February 2014
Available online 17 February 2014

Keywords:
Thymidylate kinase
Drug target
Brugia malayi
Substrate specificity
Enzyme inhibition
Homology modelling and docking

ABSTRACT

Thymidylate kinase (TMK) is a potential chemotherapeutic target because it is directly involved in the synthesis of deoxythymidine triphosphate, which is an essential component for DNA synthesis. The gene encoding thymidylate kinase of *Brugia malayi* was amplified by PCR and expressed in *Escherichia coli*. The native molecular weight of recombinant *B. malayi* thymidylate kinase (rBmTMK) was estimated to be ~52 kDa by gel filtration chromatography, suggesting a homodimeric structure. rBmTMK activity required divalent cation and Mg^{2+} was found to be the most effective cation. The enzyme was sensitive to pH and temperature, it showed maximum activity at pH 7.4 and 37 °C. The K_m values for dTMP and ATP were 17 and 66 μM, respectively. The turnover number k_{cat} was found to be 38.09 s^{-1}, a value indicating the higher catalytic efficiency of the filarial enzyme. The nucleoside analogues 5-bromo-2′-deoxyuridine (5-BrdU), 5-chloro-2′-deoxyuridine (5-CldU) and 3′-azido-3′-deoxythymidine (AZT) showed specific inhibitory effect on the enzyme activity and these effects were in good association with binding interactions and the scoring functions as compared to human TMK. Differences in kinetic properties and structural differences in the substrate binding site of BmTMK model with respect to human TMK can serve as basis for designing specific inhibitors against parasitic enzyme.

1. Introduction

Lymphatic filariasis (LF) is a debilitating helminthic disease caused by *Wuchereria bancrofti* and *Brugia* sp., over 120 million people in the world are currently infected and about 40 million of them are disfigured and incapacitated. Most of the infections of the LF are asymptomatic and show no external signs of the infection but these asymptomatic infections still cause damage to lymphatic system and kidneys along with this also affects the immune system of the host (WHO factsheet 102, January 2012). The current treatment for filariasis is based on limited number of drugs such as diethylcarbamazine (DEC), albendazole and ivermectin. These drugs alone or in combination presently being used to control the filarial infection, are microfilaricidal in nature showing little effect on the adult parasites (Critchley et al., 2005; Ramzy et al., 2006; Hoerauf, 2006). The indications of resistance have been also reported for albendazole and ivermectin (Osei-Atweneboana et al., 2007; Schwab et al., 2007). For the development of a parasite inhibitory drug, identification and characterization of targets which are present in the parasite but absent in humans is required. Nevertheless, even if a target is common to both parasite and host, slight structural differences may enhance the optimization of a new drug (Fidock et al., 2004). The enzymes of nucleic acid metabolism serve as potential drug targets due to their indispensable role in the DNA and RNA metabolism. Thymidylate kinase (thymidine monophosphate kinase, dTMP kinase, deoxythymidine monophosphate kinase, ATP: TMP phosphotransferase, EC 2.7.4.9) belongs to the NMP kinase super-family and is critical for the synthesis of deoxythymidine triphosphate (dTTP). In contrast to other nucleoside monophosphate kinases (NMPKs), TMK is cell-cycle regulated with its expression limited to the S-phase of cell replication (Su and Sclafani, 1991; Liang et al., 1995). The enzyme catalyzes the reversible phosphorylation of deoxythymidine monophosphate (dTMP) to its diphosphate form deoxythymidine diphosphate

* Corresponding author. Tel.: +91 522 2625932; fax: +91 522 2623405.
E-mail address: jkscdri@yahoo.com (J.K. Saxena).

http://dx.doi.org/10.1016/j.actatropica.2014.02.003
0001-706X/

(dTDP) in the presence of Mg^{2+} with ATP as the phosphate donor (Li de la Sierra et al., 2001). TMK is found in all organisms for de novo pyrimidine synthesis and crystal structures of the TMK from a number of species have been determined (Li de la Sierra et al., 2001; Lavie et al., 1997, 1998a; Ostermann et al., 2000a; Kotaka et al., 2006). The protein is a homodimer containing five-stranded parallel β-sheets surrounded by 7–11 α-helices in each subunit. The substrate binds in the groove on the surface of the subunit, which is characterized by three conserved sequence motifs containing structural elements required for substrate recognition and catalysis. The first is highly conserved 'P-loop' motif with consensus sequence G(X)4GKS/T, residues 13–17 in human which binds with the α- and β-phosphoryl groups of the phosphoryl donor (ATP) through interactions between amide backbone hydrogens and phosphate oxygen atoms. The second critical loop contains the DR(Y/H) motif which is a characteristic of TMPKs (Saraste et al., 1990; Ostermann et al., 2000b; Reynes et al., 1996). The third is LID region (residues 135–150 in human), which is a flexible stretch that partially encloses the phosphoryl donor when it binds and is implicated in the catalysis (Ostermann et al., 2000b).

The location of TMK at the junction of the de novo and salvage pathways for dTTP synthesis makes it a regulatory enzyme for the synthesis of DNA and therefore essential for cell growth and survival (Ostermann et al., 2000b; Anderson, 1973). TMK is well recognized as a potential drug target, with the most notable function being in the activation of anti-HIV nucleoside prodrugs (Jacobsson et al., 1998). Many studies have been conducted to develop the inhibitor against parasite specific TMKs. For eukaryotic parasites, most of the inhibitor studies have been conducted against *Plasmodium falciparum* TMK (PfTMK). Carbocyclic nucleoside analogues, modified thymine base analogues and thymidine urea derivatives have been tested for inhibitory effect on PfTMK (Kato et al., 2012; Kandeel et al., 2009; Cui et al., 2012). In case of prokaryotic TMKs various compounds such as modified thymine base, 3′ substituted nucleosides and nucleotides, 2′,3′ bicyclic analogues, thymidine 5′-O-monophosphate analogues, substituted benzyl thymine analogues and acyclic nucleoside analogues were tested against *Mycobacterium tuberculosis* (Pochet et al., 2003; Vanheusden et al., 2002, 2003; Vanheusden et al., 2004; Van Daele et al., 2006; Gasse et al., 2007; Familiar et al., 2008). Piperidinylthymine analogues were found to be active against *Staphylococcus aureus* TMK and a commercially available compound 1-methyl-6-phenyl imidazopyrinon and its derivatives inhibited *Pseudomonas aeruginosa* TMK at nanomolar concentration (Martinez-Botella et al., 2012; Choi et al., 2012). Recently TMPK has been validated as a drug target in gram-positive bacterium Staphylococcus aureus (Keating et al., 2012). The present paper reports the cloning, expression and kinetic characterization of *Brugia malayi* thymidylate kinase. The comparison of kinetic properties with the other parasites and human enzyme showed characteristic differences in the properties of the enzyme. These differences may serve the basis of designing of new chemotherapeutic compounds.

2. Materials and methods

2.1. Materials

Lactate dehydrogenase, pyruvate kinase and protein molecular weight standards were purchased from Sigma (St. Louis, MO, USA). Anti-His IgG, Ni-NTA agarose and Gel elution kit were purchased from Qiagen (Germany). IPTG, prestained markers, restriction enzymes (*EcoRI* and *XhoI*), cDNA synthesis kit and T4 ligase were purchased from MBI Fermentas (Hanover, MD, USA). Sephadex 200HR gel filtration column was purchased from GE Healthcare. pET28a (+) expression vector was purchased from Novagen (Madison, WI, USA). pGEMT cloning vector and Taq DNA polymerase were purchased from Promega (Madison, WI, USA).

2.2. Phylogenetic analysis and sequence comparison

Sequences of TMKs from different prokaryotic and eukaryotic sources including *B. malayi* were obtained from NCBI protein database (http://www.ncbi.nlm.nih.gov/protein) and used for multiple sequence alignment with clustalW programme (ftp://ftp.ebi.ac.uk/pub/software/clustalw2) and ESPript 2.2 web tool (http://espript.ibcp.fr/ESPript/ESPript) (Larkin et al., 2007; Gouet et al., 1999). A phylogenetic tree was generated by using the same sequences with the help of programme Mega5 (Tamura et al., 2011).

2.3. cDNA synthesis, polymerase chain reaction and cloning

Total RNA of *B. malayi* was isolated by Trizol method and the quality of isolated RNA was checked on 1.0% (w/v) agarose gel, undegraded RNA preparation showing two distinct bands of 28 s and 18 s was used for reverse transcription reaction as reported earlier by Singh et al. (2008). About 20 ng RNA was subjected to cDNA synthesis using cDNA synthesis kit. PCR amplification of *B. malayi tmk* gene was done by using the forward primer 5′-GAA TTC ATG GGA TCA CGA ATA CGC GGA G-3′ (*EcoRI* site under lined) and the reverse primer 5′-CTC GAG GAG GAA CAT AAG GCT CTT TCT G-3′ (*XhoI* site under lined). Primers were designed on the basis of sequence information available at http://www.ncbi.nlm.nih.gov/gene. PCR reaction was carried out in 50 μl reaction mixture consisting of 1× PCR buffer, 200 μM dNTPs, 10 pmol of each primer, 1.5 mM $MgCl_2$, 20–50 ng cDNA and 1.0 U of Taq DNA polymerase. The PCR reaction was performed for 30 cycles: 30 s at 94 °C, 90 s at 56 °C, 2 min at 72 °C in a thermocycler (PTC-100 MJ Research, USA). PCR amplified product was cloned into pGEMT cloning vector. The gene was digested out from the plasmid with restriction endonucleases *EcoRI* and *XhoI* and subcloned into a prokaryotic expression vector pET28a (+) resulting in plasmid pET-BmTMK. This plasmid was transformed in T7 RNA polymerase encoding *Escherichia coli* C-41 strain. Cloning of complete BmTMK ORF was confirmed by the sequencing of the clone.

2.4. Expression and purification

The *E. coli* C-41 strain harbouring pET-BmTMK plasmid was grown overnight in Luria–Bertini (LB) medium at 37 °C, supplemented with 30 μg/ml kanamycin. 1% (v/v) of cells were inoculated into the same fresh medium and cells were grown at 37 °C to midlog phase (OD_{600} = 0.5–0.6). Induction of expression was carried out by the addition of isopropyl β-D-1-thiogalactopyranoside (IPTG) to a final concentration of 0.5 mM and cell growth was continued at 20 °C for 16 h. Cells were harvested by centrifugation at 8000 × *g* for 5 min and pellet was resuspended in lysis buffer (50 mM NaH_2PO_4, 300 mM NaCl, 10 mM imidazole) pH 8.0 containing protease inhibitor cocktail (Sigma) and lysed by pulse sonication. The insoluble debris was removed by centrifugation at 12,000 × *g* for 45 min at 4 °C. The histidine-tagged BmTMK was purified from the soluble fraction using nickle nitrilotriacetic acid (Ni^{2+}-NTA) affinity resin. The bound protein was eluted using a stepwise imidazole gradient and fractions showing enzyme activity were dialysed against 50 mM sodium phosphate buffer, pH 7.6, containing 200 mM NaCl, 1 mM EDTA, 8% glycerol and 1 mM DTT.

2.5. SDS-PAGE and Western blotting

The sub-unit molecular mass of rBmTMK was determined by 12% (w/v) SDS-PAGE according to the method of Laemmli (1970).

For western blotting rBmTMK was electro-blotted onto the nitrocellulose membrane using wet transfer method (TE 22 Mini Tank Transfer Unit, Amersham) according to the method of Sambrook et al. (1989). Membrane was blocked with 5% nonfat milk in PBS-T (50 mM NaH_2PO_4 pH 7.5, 150 mM NaCl, 0.05% (v/v) Tween 20) for 1 h and subsequently membrane was incubated with anti-His antibodies (1:1000 dilution) at room temperature for 2 h with constant shaking followed by five washings with PBS-T. Membrane was then incubated with horseradish peroxidase (HRP) conjugated anti-mouse IgG (1: 2500 dilution) for 2 h with constant shaking and 5 washings with PBS-T. The blot was developed by chromogenic peroxidase reaction with 3,3′-diamino benzidine.

2.6. Determination of molecular mass (Mr) of rBmTMK

The native molecular weight of rBmTMK was determined by gel filtration using Sephadex 200HR 10/30 column (manufacturer's limit 600 kDa) with AKTA fast performance liquid chromatography (Amersham Biosciences). The column was pre-equilibrated with extraction buffer (50 mM Sodium phosphate buffer pH 8.0 containing 200 mM NaCl and 0.01% sodium azide), at a flow rate of 1.0 ml/min. The native molecular mass of the enzyme was determined with the help of calibration curve between elution volume and log molecular mass (kDa) using marker proteins viz. ova-albumin (42.7 kDa), albumin (67 kDa), aldolase (158 kDa), apoferritin (443 kDa). The native molecular weight of rBmTMK was further confirmed by glutaraldehyde cross linking experiment (Bhatt et al., 2002).

2.7. Circular dichroism (CD) analysis

Circular dichroism spectropolarimetry was performed using 0.7 mg/ml of rBmTMK (12 μM protein concentration) in 50 mM NaH_2PO_4 and 200 mM Na_2SO_4. Protein spectra were recorded between 250 and 200 nm at 22 °C in mdeg on Jasco J810 spectropolarimeter using 0.1 cm cell. A scanning with buffer without protein was recorded under same condition to determine the background spectra. CD spectra were analyzed using the programme K2d2 (Andrade, 1993).

2.8. Thymidylate kinase assay and kinetics

The TMK activity was measured spectrophotometrically using an enzyme coupling assay (Blondin et al., 1994). The reaction mixture (1.0) ml contained 50 mM Tris–HCl (pH 7.4), 50 mM KCl, 1.0 mM phosphoenolpyruvate, 1.0 mM $MgCl_2$, 0.05 mM NADH, 2 U pyruvate kinase, 2U lactate dehydrogenase 0.05 mM dTMP and 0.5 mM ATP. The molar ratio of $MgCl_2$: ATP was kept constant at 2. The reaction was initiated by the addition of the recombinant enzyme and the decrease in absorbance at 340 nm was monitored on a thermostated UV-2450 PC spectrophotometer (Shimadzu, Japan). Enzyme activity was calculated using a molar extinction coefficient of 6.22 mM^{-1} cm^{-1}. One unit of enzyme activity is defined as the amount of enzyme catalyzing the production of 1.0 μmol nucleoside diphosphate min^{-1} under the above conditions. The K_m values for substrates dTMP and ATP were determined according to Michaelis–Menten equation. The activity of different nucleoside monophosphates (NMPs), deoxynucleoside monophosphates (dNMPs), nucleoside triphosphates (NTPs) and deoxynucleoside triphosphates dNTPS were tested as phosphate acceptors and phosphate donors. Antifilarials like albendazole, ivermectin, diethylcarbamazine (DEC), levamisole and suramin were tested against rBmTMK. Stock solutions for levamisole (100 mM), diethylcarbamazine (10 mM) and suramin (5 mM) were prepared in triple distilled water. Whereas, stock solutions for albendazole (10 mM) and ivermectin (10 mM) were prepared in dimethyl sulphoxide (DMSO). Inhibition by these compounds was measured by incubating the rBmTMK with antifilarials for 10 min prior to activity measurement. Percent inhibition data were fit to the standard IC_{50} equation to determine IC_{50} values. Product inhibition experiments were performed using different concentrations of dTDP and effect of nucleoside analogues viz. 5-bromo-2′-deoxyuridine (5-BrdU), 5-chloro-2′-deoxyuridine (5-CldU), 3′-azido-3′-deoxythymidine (AZT) was measured by incubating the enzyme with nucleoside analogues for 10 min at 25 °C. Control spectrophotometric assays were performed to verify that the compounds were inhibitors of rBmTMK and not of the coupling enzymes, by using ADP as substrate and the two coupling enzymes pyruvate kinase and lactate dehydrogenase, but no rBmTMK and dTMP (Whittingham et al., 2010). The inhibitors when used on the coupled enzymes showed no inhibitory effect at same concentration as they are specific for rBmTMK.

2.9. High performance liquid chromatography assay

HPLC assay (Haouz et al., 2003) was performed to avoid the disadvantage of the coupled enzyme on the rBmTMK activity as a function of metal ions. For the validation of the HPLC assay both dTMP and ATP were tested by spectrophotometric assay as well as HPLC assay to determine that their apparent K_m are same. The reaction was performed in 1 ml final volume of a solution containing 50 mM Tris–HCl (pH 7.4), 50 mM KCl, 2 mM MgCl2, 0.5 mM dithiothreitol and variable concentrations of dTMP and ATP. For the determination of K_m an aliquot of 100 μl was taken from reaction mixture at different times after the addition of rBmTMK, and quenched by adding 900 μl of 100 mM sodium phosphate (pH 7.0). A buffer containing 50 mM sodium phosphate, pH 6.5, 40 mM tetrabutylammonium bromide and 2.5% (v/v) ethanol was used for elution with a flow rate of 250 μl/min. The concentration of the separated nucleotides was monitored at 260 nm using Sephasil™ C18, 5-μm column (Amersham Biosciences). All the reaction velocities were calculated by monitoring the appearance of dTDP expressed in terms of optical absorbance per minute at 260 nm.

2.10. Effect of pH, temperature, monovalent metal ions and divalent metal ions

To determine optimal pH the activity was measured at different pH and effect of temperature on enzyme was measured by incubation for 20 min at different temperatures and determining the residual activity. For the determination of the effect of monovalent metal ions rBmTMK activity was measured at different concentrations of NaCl and KCl. Effect of divalent metal ions ($MgCl_2$, $MnCl_2$, $CoCl_2$, $CaCl_2$, $CuCl_2$, $ZnSO_4$ and $NiSO_4$) on rBmTMK were determined by HPLC assay. For this 2 mM of each metal ion was mixed with 1 ml of reaction mixture containing 50 mM Tris–HCl (pH 7.4), 50 mM KCl, 0.5 mM dithiothreitol, 0.05 mM dTMP, 0.5 mM ATP and rBmTMK. Concentration of separated nucleotides and activity was measured as above.

2.11. Molecular modelling and docking studies

To explore the 3D structure and substrate binding site of BmTMK, a homology model was constructed. BlastP of BmTMK sequence against PDB (http://www.rcsb.org/pdb/home/home.do) was performed to find out suitable templates. Human thymidylate kinase (HsTMK) and *P. falciparum* thymidylate kinase (PfTMK) complexed with TMP and ADP (PDB-id 1E2D and 2WWF) were selected as templates and ClustalW (www.ebi.org) was used to generate alignment between query and templates. Finally 10 models were generated using Modeller 9v10 (Eswar et al., 2006). Models were then subjected to SAVES server for structural validation. Differences

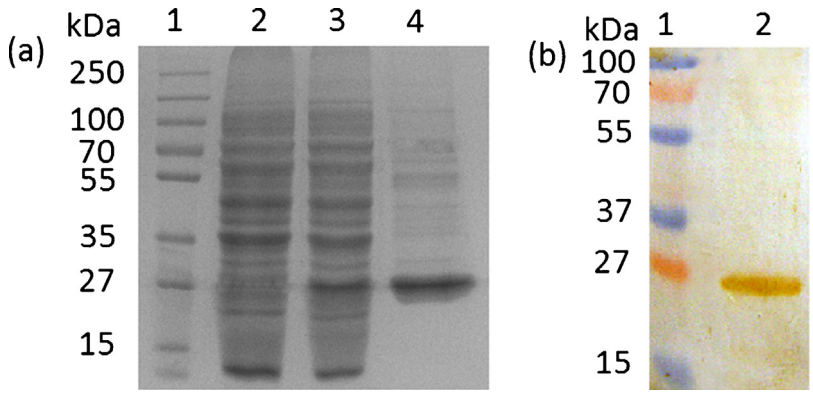

Fig. 1. Purification of rBmTMK expressed in *E. coli*. (a) 12% SDS-PAGE analysis of purified recombinant BmTMK. *E. coli* lysate expressing rBmTMK was purified by Ni-NTA affinity chromatography. *Lane 1*: Prestained protein markers, *Lane 2*: crude extract of cells harbouring recombinant plasmid without IPTG induction. *Lane 3*: crude extract of cells harbouring recombinant plasmid with IPTG induction. *Lane 4*: Purified rBmTMK eluted at 250 mM imidazole. (b) Western blot analysis using anti-His antibody as probe. *Lane 1*: Prestained protein marker. *Lane2*: purified protein.

in active site of BmTMK and HsTMK were also determined. The docking studies of the substrate dTMP and inhibitors 5-BrdU, 5-CldU and AZT was carried out by using Molegro virtual docker 4.0 and validation of docking protocol was carried out by redocking the dTMP in the same binding site of BmTMK. MolDock is a docking module of Molegro Virtual Docker (MVD) software (Thomsen and Christensen, 2006). It is based on a new hybrid search algorithm, called guided differential evolution (DE). The guided DE algorithm combines the DE optimization techniques with a cavity prediction algorithm. DE was introduced by Storn and Price in 1995 and has previously been successfully applied to molecular docking (Storn and Price, 1997). The use of predicted cavities during the search process allows for a fast and accurate identification of potential binding modes (poses). The docking scoring function of MolDock is based on a piecewise linear potential (PLP) introduced by Gehlhaar et al. (1995, 1998). In MolDock, the docking scoring function is extended with a new term, taking hydrogen bond directionality into account. Moreover, a re-ranking procedure was applied to the highest ranked poses to further increase docking accuracy. The reported crystal structure of HsTMK (PDB ID: 1E2D) was obtained from Brookhaven Protein Data Bank (PDB). Initially, the protein was considered without ligand and water molecules. The backbone was fixed, the CharmM force field and minimization using steep descent algorithm was applied for homology modelled BmTMK and all the compounds under study were prepared using the CharmM forces field and minimized up to a gradient of 0.01 kcal/(mol Å) with the help of Discovery Studio 2.0 software (Telesis Court, San Diego, CA). Due to the availability of the co-crystallized structure of HsTMK (PDB ID: 1E2D), we used the template docking available in the Molegro virtual docker and evaluated the MolDock, rerank, and protein-ligand interaction scores from MolDock [GRID] options. Template docking is based on extracting the chemical properties like the pharmacophore elements of a ligand bound in the active site. This information is utilized in the docking of the structurally similar analogues. The dTMP substrate from 1E2D was used as the template with the default settings, including a grid resolution of 0.30, for grid generation and 11 Å radius from the template as the binding site. MolDock SE was used as a search algorithm and the number of runs was set to 10. A population size of 50 and a maximum iteration of 1500 were used for parameter settings. The maximum number of poses generated was 10. Since Molegro virtual docker works by an evolutionary algorithm, consecutive docking runs do not give exactly the same pose and interactions. To address this inherent randomness, three consecutive runs were done and the top three poses were used to visualize the interactions of all inhibitors. The homology modelled protein structure as reported in the section above was used for docking experiments and the same protocol was used to validate the interactions and scoring functions in the docking experiments.

3. Results and discussion

3.1. Phylogenetic analysis and sequence comparison

Phylogenetic relationship of BmTMK with TMKs of other organisms showed that TMK is conserved in prokaryotes as well as in eukaryotes throughout the path of evolution (Supplementary Fig. 1a). TMKs from various organisms can be broadly grouped in to two categories, prokaryotic and eukaryotic forms. Among eukaryotic TMKs, BmTMK is closer to the human and *P. falciparum* TMK than yeast while BmTMK showed distant relationship with prokaryotic TMKs.

The sequence comparison of BmTMK with human, *Caenorhabditis elegans*, *W. bancrofti*, *Wolbachia*, *P. falciparum*, *M. tuberculosis*, *Streptococcus pneumoniae* and *E. coli* showed 43%, 41%, 96%, 29%, 41%, 27%, 25%, and 26% homology, respectively. BmTMK contains three conserved regions viz. phosphate binding loop (P-loop) with the conserved sequence GXXXXGK(S/T) (where X is any amino acid) between residues 14–21, general dTMP binding motif DR(Y/F/H) XXSXXA (F/Y) which is conserved between residues 97–106 and the Lid domain (Supplementary Fig. 1b). TMKs are classified into two types, on the basis of the position of active-site arginine residues (Lavie et al., 1998a). Type I TMKs have an invariant arginine residue in the P-loop but does not have such a residue in the LID domain, e.g. human and yeast TMKs. In contrast, type II TMKs lack basic residues in the P-loop and contain an arginine residue in the LID domain that is not strictly conserved, e.g. *E. coli* TMK. The result of sequence alignment of BmTMK indicated that it is closer to eukaryotic enzymes and could be classified as type I TMK.

3.2. Over-expression and purification of thymidylate kinase

According to the sequence information available at http://www.ncbi.nlm.nih.gov/gene for BmTMK specific forward and reverse primers were designed and used for the amplification of complete ORF of BmTMK by PCR, using cDNA of *B. malayi* as template. The PCR product of 642 bp was cloned into expression vector pET28a (+) and subsequent transformation of this construct in *E. coli* C-41 strain expressed a soluble protein of expected monomeric size of ~24 kDa, which was confirmed by western blotting using anti-His antibodies. N-terminal hexahistidine

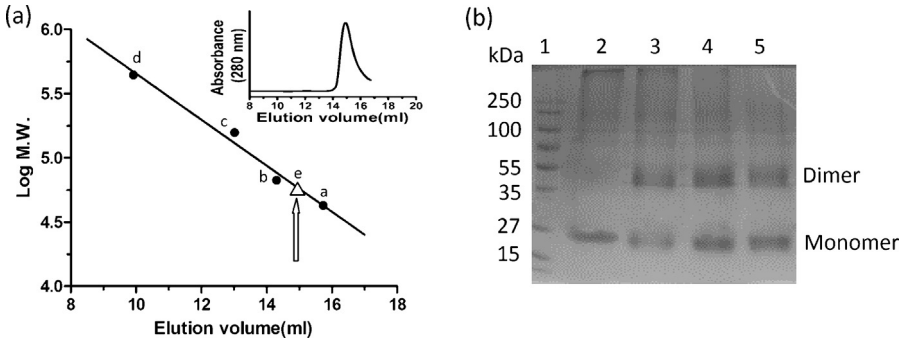

Fig. 2. Determination of molecular mass of recombinant BmTMK. (a) The native molecular mass of the protein was determined by FPLC using Sephadex 200HR 10/300 gel filtration column. The column was calibrated with molecular weight standard markers: a – Ova-albumin (42.7 kDa), b – albumin (67 kDa), c – aldolase (158 kDa), and d – apoferritin (443 kDa). Arrow indicates the native molecular mass of. Size exclusion chromatography profile of native rBmTMK with absorbance at 280 nm is shown in inset. (b) 8% SDS–PAGE profile of Glutaraldehyde cross-linked samples, *Lane 1*: molecular weight standard markers, *Lane 2*: Native rBmTMK, *Lane 3*: Cross-linked rBmTMK with 0.1% Glutaraldehyde similarly, *Lane 4 and Lane 5*: Cross-linked with 0.05% and 0.025% Glutaraldehyde.

tagged BmTMK was purified by Nickel affinity column (Ni^{2+}-NTA), by a stepwise gradient of imidazole. Highly purified protein was eluted by 250 mM imidazole (three column volumes) and the concentration was determined by Lowry et al. (1951).

Purified rBmTMK showed a single ~24 kDa band in SDS-PAGE, which was further confirmed by western blotting using anti-His antibody (Fig. 1a and b). Gel filtration of the native rBmTMK on Sephadex 200HR 10/300 gel filtration column, calibrated with standard molecular weight markers, showed a single peak with a retention volume of 14.8 ml (Fig. 2a inset). When elution volumes of marker proteins were plotted as a function of log molecular mass rBmTMK was found to have a molecular mass of about ~52 kDa suggesting the dimeric nature of the BmTMK (Fig. 2a). This is similar to TMKs from *E. coli*, *M. tuberculosis*, *P. falciparum*, yeast and human (Lavie et al., 1997, 1998a; Ostermann et al., 2000b; Munier-Lehmann et al., 2001; Whittingham et al., 2010). Dimeric nature of the BmTMK was further confirmed by interchain cross-linking of the monomeric subunits by using glutaraldehyde as cross-linker. The cross-linked dimer was then analyzed by 8% (w/v) SDS-PAGE (Fig. 2b).

3.3. Circular dichroism (CD) analysis

CD analysis of purified rBmTMK showed that α and β contents of the rBmTMK are 45% and 18%, respectively while, remaining structure is randomly coiled structure. This result closely resembles with BmTMK homology model helix contents. The α and β contents of the model protein were observed 47.4% and 15%, respectively, as predicted by the programme Prostat available with Insight 2000.1.

3.4. Effect of pH and temperature on enzyme activity

The effect of pH on enzyme activity was determined using buffers of different pH at a concentration of 50 mM and the optimum activity pH was found to be 7.4 which is similar to yeast thymidylate kinase which showed highest activity at pH 7.5, *S. pneumoniae* thymidylate kinase showed highest activity at pH 8.5 (Lavie et al., 1998b; Petit and Koretke, 2002). The activity of *P. falciparum* TMK was observed over the entire range of pH (6–10) with maximal activity between pH 7 and 9 (Kandeel and Kitade, 2008). The rBmTMK does not show activity over a wide pH range, the activity was markedly dropped on increasing or decreasing the pH above pH 8.0 and blow pH 7.0. The optimum temperature for activity was 37 °C. However rBmTMK was stable below 40 °C, the enzyme activity was decreased to 30% at 45 °C and complete inactivation at 50 °C, this study shows that rBmTMK is very sensitive to pH and temperature.

3.5. Effect of mono and divalent cations on enzyme activity

Na^+ and K^+ upto 0.5 M showed no effect on the rBmTMK activity. A divalent cation is essential for thymidylate kinase activity (Nelson and Carter, 1969). Mg^{2+} was the most favourable divalent cation and activity was not observed in the absence of Mg^{2+}. Interestingly in the presence of Co^{2+} rBmTMK showed similar activity as observed with Mg^{2+}, while Mn^{2+} and Ni^{2+} showed 52.84 and 10.25% activity, respectively. In the presence of Ca^{2+} and Cu^{2+} less than 10% activities were observed, while with Zn^{2+} it showed no activity (Table 1). Effect of divalent metal ions was determined with the help of HPLC assay (Supplementary Fig. 2a and b). In case of *E. coli* TMK Mn^{2+}, Co^{2+} and Ni^{2+} substituted Mg^{2+} by 41%, 18% and 2.2%, respectively, but it showed no activity with Zn^{2+} and Cd^{2+} (Nelson and Carter, 1969). HsTMK showed 75% activity with Mn^{2+} in comparison to Mg^{2+} but no activity was observed with Ca^{2+}, Cu^{2+}, Zn^{2+} and Fe^{2+} (Lee and Cheng, 1977). Mg^{2+} and Co^{2+} are preferred metal ions for filarial enzyme.

3.6. Kinetic studies of B. malayi thymidylate kinase

The thymidylate kinase activity was found to be sensitive to ATP/Mg^{2+} ratio. The maximal activity was achieved at equimolar concentrations of ATP and Mg^{2+}, the ratio of ATP to Mg^{2+} was maintained at 1:2 in all cases, as the ratio of complexed to free nucleotide can be expected to affect the results. The kinetics of the forward reaction (formation of dTDP and ADP) was measured by coupling the reaction with pyruvate kinase and lactate dehydrogenase. First, initial reaction rates were measured with ATP as the variable substrate (0.025–0.5 mM) and dTMP as the fixed substrate. The apparent Michaelis constant (K_m) estimated

Table 1
Effects of metal ions on recombinant BmTMK.

Metal ions (2 mM)	Activity (%)
Mg^{2+}	100.00
Co^{2+}	100.00
Mn^{2+}	52.84
Ni^{2+}	10.25
Ca^{2+}	2.94
Cu^{2+}	2.12
Zn^{2+}	0.00

The values are means of three independent experiments
Activity was measured by HPLC assay as described in Section 2.

Table 2
Kinetic properties of TMK from different sources.

Organism	K_m (μM) dTMP	K_{cat}/K_m (s^{-1} mM^{-1})	K_m (μM) ATP	K_{cat}/K_m (s^{-1} mM^{-1})	K_{cat} (s^{-1})	Reference
E. coli	2.7	5600	8	1875	15	Lavie et al. (1998a,b)
Yeast	9	3900	190	184	35	Lavie et al. (1998a,b)
P. falciparum	10.7	460	78.6	62	4.9	Whittingham et al. (2010)
H. sapiens wt	5	140	5	140	0.70	Ostermann et al. (2003)
S. pneumoniae	66	134	235	38	8.9	Petit and Koretke (2002)
M. tuberculosis	4.5	1000	100	45	4.5	Munier-Lehmann et al. (2001)
Brugia malayi	17	2240	66	577.12	38.09	Present study

by Lineweaver–Burk plot for ATP was 66 μM. K_m of thymidylate kinase with ATP from other sources ranged between 8 and 235 μM (Table 2). When dTMP used as variable substrate (0.005–0.08 mM) and ATP-Mg^{2+} concentration was fixed, the apparent K_m for dTMP was 17 μM. K_m of thymidylate kinase for dTMP from other sources has been reported between 2.7 and 66 μM (Table 2).

The k_{cat} value of rBmTMK was calculated to be 38.09 s^{-1}, showing higher catalytic efficiency of the enzyme. The k_{cat} value of HsTMK is 0.70 which is quite low in comparison to rBmTMK (Ostermann et al., 2003). The k_{cat}/K_m value of rBmTMK was found to be 2240 s^{-1} mM^{-1} for dTMP, which is lower as compared to *E. coli* and yeast TMKs but higher than *S. pneumoniae*, *M. tuberculosis*, *P. falciparum* and human TMKs. k_{cat}/K_m value for TMK with substrate dTMP in human is 140 s^{-1} mM^{-1} which is quite low in comparison to rBmTMK, this difference in the catalytic efficiency can be exploited for the development of inhibitors against filarial enzyme. The higher catalytic efficiency of the rBmTMK, might be co-related with the synthesis of DNA precursors in higher amount in the *B. malayi*. The kinetic parameters of TMK from different organisms are summarized in Table 2.

3.7. Substrate specificity

The ability of various nucleoside monophosphates to act as phosphate acceptors and nucleoside triphosphates to act as phosphate donors was determined for *B. malayi* thymidylate kinase.

Table 3
The phosphate donor activity of various nucleoside triphosphates on rBmTMK.

Substrate	Substrate conc. (mM)	Enzyme activity (%)
ATP	0.5	100.00
dATP	0.5	26.90
GTP, dGTP	0.025–5.0	0.00
CTP, dCTP	0.025–5.0	0.00
TTP, dTTP	0.025–5.0	0.00
UTP, dUTP	0.025–5.0	0.00

The nucleoside triphosphates were used at 0.025, 0.05, 0.1, 0.3, 0.5, 1.0, 2.5 and 5.0 mM concentration.
The activity was measured as reported in Section 2.

3.7.1. Phosphate donors of thymidylate kinase

ATP is the most favourable phosphate donor for thymidylate kinase reaction and some other nucleoside triphosphates may also serve as phosphate donors. In case of rBmTMK, different ribo- and deoxyribonucleoside triphosphates were tested, ATP and dATP were found to be most active as phosphate donors. dATP showed 26.9% activity at 0.5 mM concentration in comparison to ATP while no activity was observed with other NTPs (Table 3). Besides ATP and dATP, yeast TMK also utilized CTP, dCTP, GTP, dGTP, and UTP

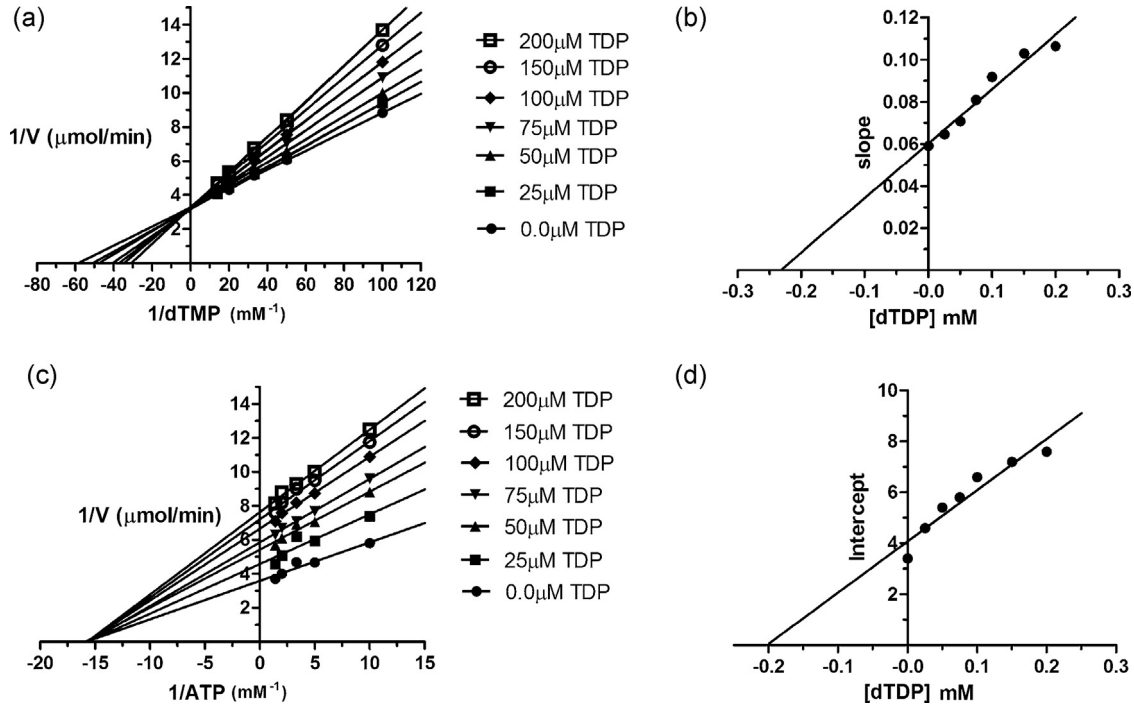

Fig. 3. Double-reciprocal plots of ATP and dTMP concentrations against the initial velocity for rBmTMK activity in presence of dTDP. (a) The concentration of ATP was held constant at 0.5 mM and the concentration of dTMP was varied. (b) The slope of the double reciprocal graph is plotted against the dTDP concentrations. (c) The concentration of dTMP was held constant at 0.05 mM and the concentration of ATP was varied. (d) The intercept of the double reciprocal graph are plotted against the dTDP concentrations. The concentrations of dTDP were 0, 25, 50, 75, 100, 150 and 200 μM in both the cases.

Table 4
The phosphate acceptor activity of various nucleoside monophosphates on rBmTMK.

Substrate	Substrate conc. (mM)	Enzyme activity (%)
TMP	0.1	100.00
dUMP	0.1	12.10
CMP	0.025–5.0	0.00
GMP	0.025–5.0	0.00
AMP	0.025–5.0	0.00
UMP	0.025–5.0	0.00
dCMP	0.025–5.0	0.00
dGMP	0.025–5.0	0.00
dAMP	0.025–5.0	0.00
dIMP	0.025–5.0	0.00

The nucleoside monophosphate was used at 0.025, 0.05, 0.1, 0.3, 0.5, 1.0, 2.5 and 5.0 mM concentration.
The enzyme activity was measured as mentioned in Section 2.

as phosphate donor showing 30–50% activity (Jong and Campbell, 1984). The *S. pneumoniae* TMK showed 80% and 20% activity with dATP and CTP, respectively (Petit and Koretke, 2002). HsTMK showed 100%, 42% and 38% activity with dATP, dGTP and GTP, respectively, while 4–12% activity was observed with CTP, dCTP, UTP and dUTP (Lee and Cheng, 1977). *P. falciparum* TMK showed 64% activity with dATP and less than 10% activity with GTP, CTP, UTP and dTTP up to 5 mM concentration (Kandeel and Kitade, 2008). *E. coli* TMK showed 80%, 31.6%, 21.3% activity with dATP, CTP, and dCTP, respectively, while 1–12% activity was observed with GTP, dGTP, UTP and dTTP (Nelson and Carter, 1969). *M. tuberculosis* TMK showed 120%, 60%, 42% and 26% activity with dATP, GTP, CTP and UTP, respectively (Munier-Lehmann et al., 2001). Thus rBmTMK is more specific for phosphate donors as compared to *E. coli*, *S. pneumoniae*, *P. falciparum*, yeast and human TMKs.

3.7.2. Phosphate acceptors of thymidylate kinase

In the present study NMPs and dNMPs were used to determine phosphate acceptor ability of rBmTMK at different concentration (0.025–5.0 mM). Among nucleoside monophosphates besides dTMP, only dUMP showed detectable 12.1% activity as compared to dTMP (Table 4). *M. tuberculosis*, *E. coli, S. pneumonia* and yeast TMK utilized dTMP as phosphate acceptor while with dUMP these enzymes showed 33%, 14.7%, 15% and 31% activity, respectively. In comparison to dTMP other NMPs were not active as a phosphate acceptors for these parasites (Munier-Lehmann et al., 2001; Petit and Koretke, 2002; Nelson and Carter, 1969; Jong and Campbell, 1984). *P. falciparum* TMK showed 43% activity with dUMP, it also showed 86, 15 and 1.3% activity with dGMP, dIMP and GMP, respectively (Kandeel and Kitade, 2008). However HsTMK showed activity only with dTMP. The above results suggested that rBmTMK is more specific than *E. coli*, *S. pneumoniae*, yeast and *P. falciparum* TMKs for the phosphate acceptors.

In case *P. falciparum*, TMK utilizes both purine and pyrimidine nucleosides as phosphate acceptor while human HsTMK can only accommodate pyrimidine nucleosides, although its folded structure and active site are very similar to HsTMK. The difference in utilization of phosphate acceptors may be due to presence of some smaller residues (Glu68, Ala111 and Thr158) in the substrate binding pocket as compared to HsTMK (Kandeel and Kitade, 2008). HsTMK active site cavity is very narrow and rigid, so it can accommodate only pyrimidine nucleosides (Lavie et al., 1997; Kenyon, 1997). In our experiments we observed that rBmTMK utilizes only pyrimidine nucleosides as phosphate acceptor (Table 4). When the active sites of human and *B. malayi* TMK were compared no significant differences in the size of the substrate binding pocket residues were observed.

Table 5
IC50 values of some antifilarial compounds against BmTMK.

Antifilarials	IC_{50} (μM)
Albendazole	140
Ivermectin	150
Levamisole	1210
Diethylcarbamazine	750
Suramin	18

Activity was measured as reported in Section 2.

3.8. Inhibition of thymidylate kinase

Different antifilarials showed varying degree of rBmTMK inhibition (Table 5). Among antifilarials tested only suramin showed significant inhibition. dTDP the product of enzyme reaction significantly inhibited the enzyme activity. When dTMP was used as a variable substrate, dTDP showed competitive inhibition with K_i value 230 μM (Fig. 3a and b). When ATP was used as a variable

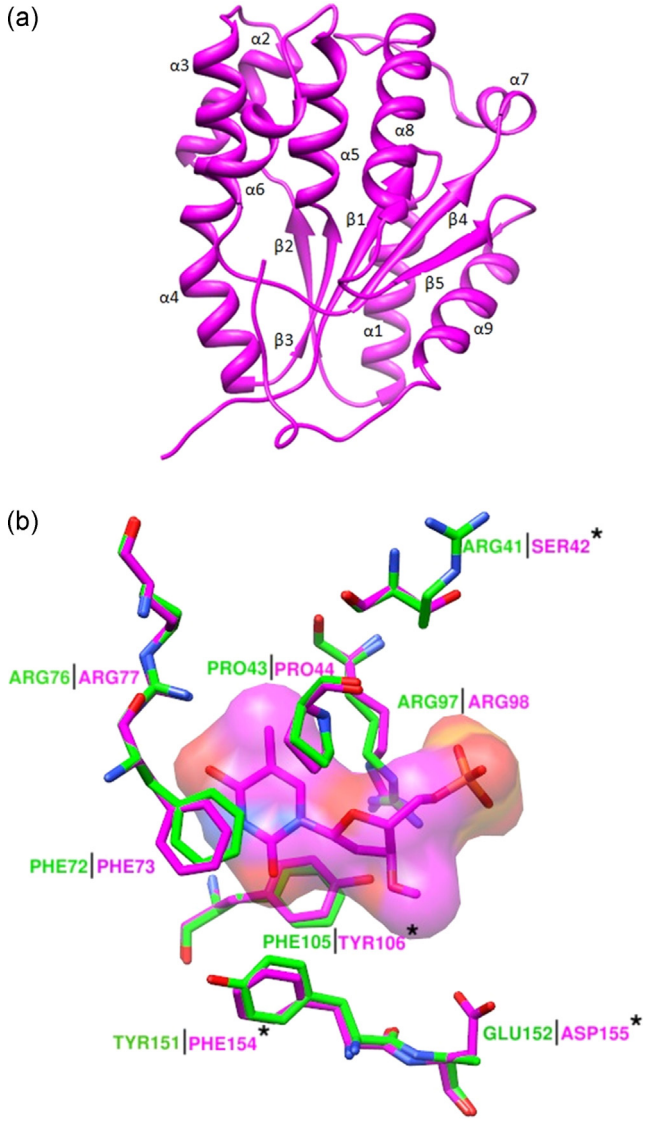

Fig. 4. Structural analysis of BmTMK. (a) 3D structure of *Brugia malayi* thymidylate kinase generated with the help of Modeller 9v10. (b) Superimposed 3D structure of BmTMK (magenta) with docked dTMP and HsTMK (green). dTMP is shown in stick and transparent surfaces. Residues of BmTMK which differs from HsTMK are marked by asterisk (*). Important residues within 6.7 Å radius around dTMP are shown for clear representation.

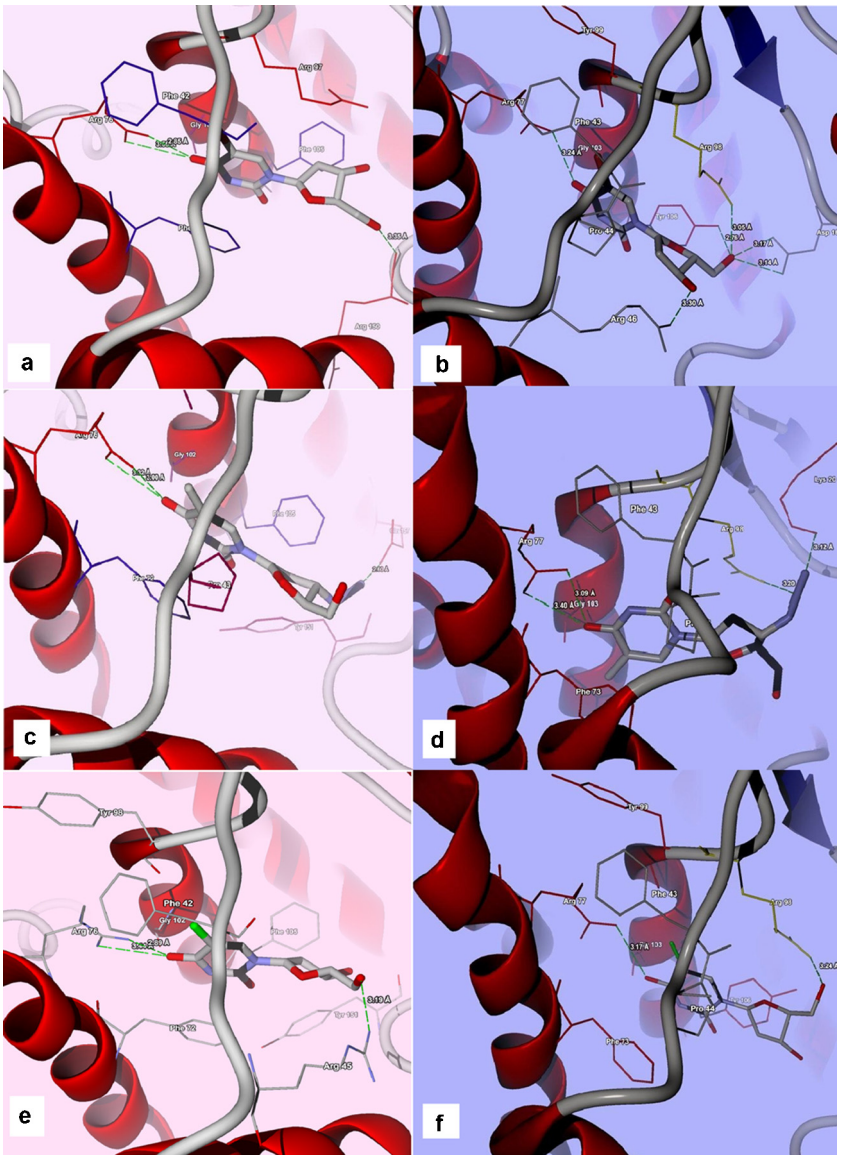

Fig. 5. The comparative binding interactions of the nucleoside analogues with BmTMK and HsTMK. 5-BrdU (a and b), AZT (c and d) and 5CldU (e and f). The interactions of BmTMK were represented in blue background while with HsTMK in pink background.

substrate a non-competitive inhibition with K_i value 212 μM was observed (Fig. 3c and d). Inhibitory effect of nucleoside analogues 5-BrdU, 5-CldU and AZT on rBmTMK was studied and compared with HsTMK. The nucleoside analogues significantly inhibited the filarial enzyme as compared to HsTMK (Table 6). Nucleoside analogues such as acyclovir, ganciclovir, zidovudine and stavudine have strong antiviral properties and are successfully being used in the treatment of HIV or herpes virus infections. The most frequently used compounds are derivatives of guanine (acyclovir, ganciclovir) or 5′-substituted pyrimidines (brivudin, idoxuridine, trifluridine) (De Clercq, 2001). When these compounds are administered as prodrugs, they are phosphorylated by cellular or viral kinases and the resulting nucleoside triphosphates have been shown to inhibit viral DNA synthesis by different mechanisms (De Clercq, 2002). Thymidine kinase (TK) and Thymidylate kinase (TMK) are involved in the first two steps of activation of prodrugs. In case of *M. tuberculosis* TK is absent and activation of prodrugs does not occur, so initially it was thought that TMK could not serve as a drug target but it has been shown that 5-bromo-2′-deoxyuridine (5-BrdU) and 3′-azido-3′-deoxythymidine (AZT) act as potent inhibitors of MtTMK,

Table 6
The comparative effect of nucleoside analogues on rBmTMK and HsTMK.

Nucleoside analogues	(HsTMK)[a] K_i (μM)	(BmTMK) K_i (μM)	Molegro docking scores on HsTMK		Molegro docking scores on BmTMK	
			Moldock score	Rerank score	Moldock score	Rerank score
5-CldU	375	42	−106.56	−84.63	−113.53	−85.3316
5-BrdU	214	20	−108.15	−88.60	−129.15	−93.2846
AZT	450	24	−114.71	−82.82	−116.46	−87.4287

Different concentrations of Nucleoside analogues were tested with variable concentration of dTMP.
[a] Results were from Pochet et al. (2003).

indicating that no metabolic processing is necessary for these compounds to become pharmacologically active unlike in the treatment of anti-herpes virus infections, these compounds could directly act on their target (Saito and Tomioka, 1984; Cole et al., 1998; Pochet et al., 2002). The study with rBmTMK showed that pyrimidine based nucleoside analogues in their non-phosphorylated form (5-BrdU, 5-CldU and AZT) significantly inhibited rBmTMK activity as compared to HsTMK suggesting that these nucleoside analogues and their derivatives may be utilize as inhibitors of BmTMK (Pochet et al., 2003). Inhibitory effect of these compounds on rBmTMK as compare to HsTMK was further validated by docking study.

3.9. Molecular modelling and docking studies

BmTMK shares 43% and 41% identity with HsTMK and PfTMK, which we found sufficient to deduce the structural information (Fig. 4a). The generated model showed 93.1%, 6.4%, 0.0% and 0.5% residues in core, allowed, generously allowed and disallowed region, respectively. Ramachandran plot showed that Arg98 was the only residue which occupies disallowed region and this residue plays important role in binding of dTMP. We did not performed optimization of loop harbouring Arg98, because corresponding residue in the templates was also in disallowed region due to unusual phi and psi angle acquired during dTMP binding (Ostermann et al., 2000b). Structural superimposition with HsTMK revealed that BmTMK has identical fold, consisting of 9 alpha helices and 5 beta sheets connected by turn(s)/loop(s). From the view of drug designing we were more interested in finding out differences in substrate binding pocket as compared to HsTMK, as this difference can be exploited to design specific inhibitory molecule against BmTMK. Interestingly we found that in the dTMP binding pocket of BmTMK Ser42, Tyr106, Phe154 and Asp155 replaced the Arg41, Phe105, Tyr151 and Glu152 of HsTMK, respectively (Fig. 4b). The effect of these substitution cannot be explained by just rigid model, but we can hypothesized that specificity can be imparted to the prospective BmTMK inhibitors. Docking simulation study of dTMP produced a conformation close to co-crystallized conformation as observed in HsTMK, suggesting a conserved binding mode of the substrate. Side chain of Arg98 and Arg77 were involved in hydrogen bonding with phosphate moiety of dTMP and keto group of thymine ring. Possible hydrophobic stacking interaction was observed between thymine ring and side chain of Phe73. In order to validate the selectivity of the nucleoside analogues 5-CldU, 5-BrdU and AZT for rBmTMK comparative docking studies with substrate dTMP were carried out. The docking studies clearly supported the observations that these compounds selectively inhibited the BmTMK instead of HsTMK (PDB ID: 1E2D). The comparative docking scores and their in vitro K_i are shown in Table 6. To further validate these results the molecular interactions of these molecules at receptor binding site were studied. Binding site interactions clearly showed that the 5-BrdU showed important interactions with amino acids viz. Arg-77, Arg-98, Tyr-106 along with the additional interactions with the amino acids viz. Arg-46 and Asp-16 these interactions may contribute for the higher binding scores and affinities for filarial enzyme than the HsTMK. In case of HsTMK it showed interactions with Arg-76 and Arg-150 which might decreases its binding affinity (Fig. 5a and b). AZT showed hydrogen bond interactions with the Arg-77, Arg-98 and Lys-20 in the BmTMK while with the HsTMK it showed interactions with the Arg-76 and Gln-157 missing the important binding interactions with Arg-97 (Fig. 5c and d). In the same manner the 5-ClDU showed interactions with Arg-77 and Arg-98 which might be the reason for low K_i values and binding scores, while with the HsTMK it showed interactions with the Arg-76 and Arg-45 missing the important binding interactions with Arg-97 (Fig. 5e and f). Hence inhibitors based on modified pyrimidine nucleosides will be highly selective against human filarial parasites.

4. Conclusion

In the present study *B. malayi* gene encoding thymidylate kinase was successfully cloned, expressed and characterized. rBmTMK, a dimeric protein, showed low sequence homology with its human host and can be categorized into Type I TMK on the basis of active site arginine residue. Results of substrate specificity showed that it can utilize only pyrimidine nucleosides as phosphate acceptor. Pyrimidine based nucleoside analogues showed selective inhibition of the rBmTMK, furthermore these results were also supported by docking studies. Significant differences in the kinetic properties and the dTMP binding pocket of BmTMK as compared to HsTMK may be exploited in parasite specific drug designing.

Acknowledgements

We gratefully acknowledge the Council of Scientific and Industrial Research (CSIR), New Delhi, for providing Junior and Senior Research Fellowship to Pawan Kumar Doharey to carry out this work. The authors are thankful to Dr. T.K. Chakraborty, Director, CDRI for his invaluable support. Communication number 8625.

Appendix A. Supplementary data

Supplementary material related to this article can be found, in the online version, at http://dx.doi.org/10.1016/j.actatropica.2014.02.003.

References

Anderson, E.P., 1973. Nucleoside and nucleotide kinases. In: Boyer, P.D. (Ed.), The Enzymes. Academic Press, New York, pp. 49–96.
Andrade, M.A., 1993. Evaluation of secondary structure of proteins from UV circular dichroism spectra using an unsupervised learning neural network. Protein Eng. 6, 383–390.
Bhatt, A.N., Prakash, K., Subramanya, H.S., Bhakuni, V., 2002. Different unfolding pathways for mesophilic and thermophilic homologues of serine hydroxymethyltransferase. Biochemistry 41, 12115–12123.
Blondin, C., Serina, L., Weismuller, L., Gilles, A.M., Barzu, O., 1994. Improved spectrophotometric assay of nucleoside monophosphate kinase activity using the pyruvate kinase/lactate dehydrogenase coupling system. Anal. Biochem. 220, 219–221.
Choi, J.Y., Plummer, M.S., Starr, J., Desbonnet, C.R., Soutter, H., Chang, J., Miller, J.R., Dillman, K., Miller, A.A., Roush, W.R., 2012. Structure guided development of novel thymidine mimetics targeting *Pseudomonas aeruginosa* thymidylate kinase: from hit to lead generation. J. Med. Chem. 55 (2), 852–870.
Cole, S.T., Brosch, R., Parkhill, J., Garnier, T., Churcher, C., Harris, D., Gordon, S.V., Eiglmeier, K., Gas, S., Barry III, C.E., Tekaia, F., Badcock, K., Basham, D., Brown, D., Chillingworth, T., Connor, R., Davies, R., Devlin, K., Feltwell, T., Gentles, S., Hamlin, N., Holroyd, S., Hornsby, T., Jagels, K., Barrell, B.G., 1998. Deciphering the biology of *Mycobacterium tuberculosis* from the complete genome sequence. Nature 393, 537–544.
Critchley, J., Addiss, D., Ejere, H., Gamble, C., Garner, P., Gelband, H., 2005. Albendazole for the control and elimination of lymphatic filariasis: systematic review. Trop. Med. Int. Health 10, 818–825.
Cui, H.Q., Carrero-Lerida, J., Silva, A.P., Whittingham, J.L., Brannigan, J.A., Ruiz-Perez, L.M., Read, K.D., Wilson, K.S., Gonzalez-Pacanowska, D., Gilbert, I.H., 2012. Synthesis and evaluation of alpha-thymidine analogues as novel antimalarials. J. Med. Chem. 55 (24), 10948–10957.
De Clercq, E., 2001. Antiviral drugs: current state of the art. J. Clin. Virol. 22, 73–89.
De Clercq, E., 2002. Strategies in the design of antiviral drugs. Nat. Rev. Drug Discov. 1, 13–25.
Eswar, N., Webb, B., Marti-Renom, M.A., Madhusudhan, M.S., Eramian, D., Shen, M.Y., Pieper, U., Sali, A., 2006. Comparative protein structure modeling using Modeller. Curr. Protoc. Bioinformatics, 6 (chapter 5, unit 5).
Familiar, O., Munier-Lehmann, H., Negri, A., Gago, F., Douguet, D., Rigouts, L., Hernandez, A.I., Camarasa, M.J., Perez-Perez, M.J., 2008. Exploring acyclic nucleoside analogues as inhibitors of *Mycobacterium tuberculosis* thymidylate kinase. ChemMedChem 3 (7), 1083–1093.
Fidock, D.A., Rosenthal, P.J., Croft, S.L., Brun, R., Nwaka, S., 2004. Antimalarial drug discovery: efficacy models for compound screening. Nat. Rev. Drug Discov. 3, 509–520.

Gasse, C., Huteau, V., Douguet, D., Munier-Lehmann, H., Pochet, S., 2007. A new family of inhibitors of *Mycobacterium tuberculosis* thymidine monophosphate kinase. Nucleos. Nucleot. Nucleic Acids 26 (8–9), 1057–1061.

Gehlhaar, D.K., Bouzida, D., Rejto, P.A., 1998. Fully automated and rapid flexible docking of inhibitors covalently bound to serine proteases in evolutionary programming. In: Proceedings of the Seventh International Conference on Evolutionary Programming, Springer, London, UK, pp. 449–461.

Gehlhaar, D.K., Verkhivker, G.M., Rejto, P.A., Sherman, C.J., Fogel, D.B., Fogel, L.J., Freer, S.T., 1995. Molecular recognition of the inhibitor AG-1343 by HIV-1 protease: conformationally flexible docking by evolutionary programming. Chem. Biol. 2, 317–324.

Gouet, P., Courcelle, E., Stuart, D.I., Metoz, F., 1999. ESpript: analysis of multiple sequence alignments in PostScript. Bioinformatics 15, 305–308.

Haouz, A., Vanheusden, V., Munier-Lehmann, H., Froeyen, M., Herdewijn, P., Van Calenbergh, S., Delarue, M., 2003. Enzymatic and structural analysis of inhibitors designed against *Mycobacterium tuberculosis* thymidylate kinase: new insights into the phosphoryl transfer mechanism. J. Biol. Chem. 14, 4963–4971.

Hoerauf, A., 2006. New strategies to combat filariasis. Expert Rev. AntiInfect. Ther. 4, 211–222.

Jacobsson, B., Britton, S., Tornevik, Y., Eriksson, S., 1998. Decrease in thymidylate kinase activity in peripheral blood mononuclear cells from HIV-infected individuals. Biochem. Pharmacol. 56, 389–395.

Jong, A.Y.S., Campbell, J.L., 1984. Characterization of *Saccharomyces cerevisiae* thymidylate kinase, the CDC8 gene product. J. Biol. Chem. 259, 14394–14398.

Kandeel, M., Ando, T., Kitamura, Y., Abdel-Aziz, M., Kitade, Y., 2009. Mutational, inhibitory and microcalorimetric analyses of *Plasmodium falciparum* TMP kinase: implications for drug discovery. Parasitology 136 (1), 11–25.

Kandeel, M., Kitade, Y., 2008. Molecular characterization, heterologous expression and kinetic analysis of recombinant *Plasmodium falciparum* thymidylate kinase. J. Biochem. 144, 245–250.

Kato, A., Yasuda, Y., Kitamura, Y., Kandeel, M., Kitade, Y., 2012. Carbocyclic thymidine derivatives efficiently inhibit *Plasmodium falciparum* thymidylate kinase (PfTMK). Parasitol. Int. 61 (3), 501–503.

Keating, T.A., Newman, J.V., Olivier, N.B., Otterson, L.G., Andrews, B., Boriack-Sjodin, P.A., Breen, J.N., Doig, P., Dumas, J., Gangl, E., Green, O.M., Guler, S.Y., Hentemann, M.F., Joseph-McCarthy, D., Kawatkar, S., Kutschke, A., Loch, J.T., McKenzie, A.R., Pradeepan, S., Prasad, S., Martínez-Botella, G., 2012. In vivo validation of thymidylate kinase (TMK) with a rationally designed, selective antibacterial compound. ACS Chem. Biol. 7, 1866–1872.

Kenyon, G.L., 1997. AZT monophosphate knocks thymidylate kinase for a loop. Nat. Struct. Biol. 4, 595–597.

Kotaka, M., Dhaliwal, B., Ren, J., Nichols, C.E., Angell, R., Lockyer, M., Hawkins, A.R., Stammers, D.K., 2006. Structures of *S. aureus* thymidylate kinase reveal an atypical active site configuration and an intermediate conformational state upon substrate binding. Protein Sci. 15, 774–784.

Laemmli, U.K., 1970. Cleavage of structural proteins during the assembly of the head of bacteriophage T4. Nature 277, 680–685.

Larkin, M.A., Blackshields, G., Brown, N.P., 2007. Clustal W and clustal X version 2.0. Bioinformatics 23, 2947–2948.

Lavie, A., Conard, M., Brundiers, R., Goody, R.S., Schlichting, I., Reinstein, J., 1998b. Crystal structure of yeast thymidylate kinase complexed with the bisubstrate inhibitor P1-(5′-adenosyl) P5-(5′-thymidyl) pentaphosphate (TP5A) at 2. 0 Å resolution: implications for catalysis and AZT activation. Biochemistry 37, 3677–3686.

Lavie, A., Ostermann, N., Brundiers, R., Goody, R.S., Reinstein, J., Konrad, M., Schlichting, I., 1998a. Structural basis for efficient phosphorylation of 3-azidothymidine monophosphate by *Escherichia coli* thymidylate kinase. Proc. Natl. Acad. Sci. U. S. A 95, 14045–14050.

Lavie, A., Vetter, I.R., Konrad, M., Goody, R.S., Reinstein, J., Schlichting, I., 1997. Structure of thymidylate kinase reveals the cause behind the limiting step in AZT activation. Nat. Struct. Biol. 4, 601–604.

Lee, L.S., Cheng, Y.C., 1977. Human thymidylate kinase purification, characterization and kinetic behavior of the thymidylate kinase derived from chronic myelocytic leukemia. J. Biol. Chem. 252, 5686–5691.

Li de la Sierra, I., Munier-Lehmann, H., Gilles, A.M., Barzu, O., Delarue, M., 2001. X-ray structure of TMP kinase from *Mycobacterium tuberculosis* complexed with TMP at 1.95 Å resolution. J. Mol. Biol. 311, 87–100.

Liang, P., Averboukh, L., Zhu, W., Haley, T., Pardee, A.B., 1995. Molecular characterization of the murine thymidylate kinase gene. Cell Growth Differ. 6, 1333–1338.

Lowry, O.H., Rosebrough, N.J., Farr, A.L., Randall, R.J., 1951. Protein measurement with the Folin phenol reagent. J. Biol. Chem. 193, 265–275.

Martinez-Botella, G., Breen, J.N., Duffy, J.E., Dumas, J., Geng, B., Gowers, I.K., Green, O.M., Guler, S., Hentemann, M.F., Hernandez-Juan, F.A., 2012. Discovery of selective and potent inhibitors of Gram-positive bacterial thymidylate kinase (TMK). J. Med. Chem. 5 (22), 10010–10021.

Munier-Lehmann, H., Chaffotte, A., Pochet, S., Labesse, G., 2001. Thymidylate kinase of *Mycobacterium tuberculosis*: a chimera sharing properties common to eukaryotic and bacterial enzymes. Protein. Sci. 10, 1195–1205.

Nelson, D.J., Carter, C.E., 1969. Purification and characterization of thymidine 5′-monophosphate kinase from *Escherichia coli* B. J. Biol. Chem. 244, 5254–5262.

Osei-Atweneboana, M.Y., Eng, J.K., Boakye, D.A., Gyapong, J.O., Prichard, P.K., 2007. Prevalence and intensity of *Onchocerca volvulus* infection and efficacy of ivermectin in endemic communities in Ghana: a two-phase epidemiological study. Lancet 369, 2021–2029.

Ostermann, N., Lavie, A., Padiyar, S., Brundiers, R., Veit, T., Reinstein, J., Goody, R.S., Konrad, M., Schlichting, I., 2000a. Potentiating AZT activation: structures of wild-type and mutant human thymidylate kinase suggest reasons for the mutants' improved kinetics with the HIV prodrug metabolite AZTMP. J. Mol. Biol. 304, 43–53.

Ostermann, N., Schlichting, I., Brundiers, R., Konrad, M., Reinstein, J., Veit, T., Goody, R.S., Lavie, A., 2000b. Insights in to the phosphoryltransfer mechanism of human thymidylate kinase gained from crystal structures of enzyme complexes along the reaction coordinate. Structure 8, 629–642.

Ostermann, N., Segura-Pena, D., Meier, C., Veit, T., Monnerjahn, C., Konrad, M., Lavie, A., 2003. Structures of human thymidylate kinase in complex with prodrugs: implications for the structure-based design of novel compounds. Biochemistry 42, 2568–2577.

Petit, C.M., Koretke, K.K., 2002. Characterization of *Streptococcus pneumoniae* thymidylate kinase: steady state kinetics of the forward reaction and isothermal titration calorimetry. Biochem. J. 363, 825–831.

Pochet, S., Dugue, L., Douguet, D., Labesse, G., Munier-Lehmann, H., 2002. Nucleosides analogues as inhibitors of thymidylate kinases: possible therapeutic applications. ChemBioChem 3, 108–110.

Pochet, S., Dugue, L., Labesse, G., Delepierre, M., Munier-Lehmann, H., 2003. Comparative study of purine and pyrimidine nucleoside analogues acting on the thymidylate kinases of *Mycobacterium tuberculosis* and of humans. ChemBioChem 4, 742–747.

Ramzy, R.M., El Setouhy, M., Helmy, H., Ahmed, E.S., Abd Elaziz, K.M., Farid, H.A., Shannon, W.D., Weil, G.J., 2006. Effect of yearly mass drug administration with diethylcarbamazine and albendazole on bancroftian filariasis in Egypt: a comprehensive assessment. Lancet 367, 992–999.

Reynes, J.P., Tiraby, M., Baron, M., Drocourt, D., Tiraby, G., 1996. *Escherichia coli* thymidylate kinase: molecular cloning, nucleotide sequence and genetic organization of the corresponding tmk locus. J. Bacteriol. 178, 2804–2812.

Saito, H., Tomioka, H., 1984. Thymidine kinase of bacteria: activity of the enzyme in *Actinomycetes* and related organisms. J. Gen. Microbiol. 130, 1863–1870.

Sambrook, J., Fritsch, E.E., Maniatis, T., 1989. Molecular Cloning: A Laboratory Manual, second ed. Cold Spring Harbor Laboratory Press, New York.

Saraste, M., Sibbald, P.R., Wittinghofer, A., 1990. The P-loop: a common motif in ATP-binding and GTP-binding proteins. Trends Biochem. Sci. 15, 430–434.

Schwab, A.E., Churcher, T.S., Schwab, A.J., Basanez, M.G., Prichard, R.K., 2007. An analysis of the population genetics of potential multi-drug resistance in *Wuchereria bancrofti* due to combination chemotherapy. Parasitology 134, 1025–1040.

Singh, A.R., Joshi, S., Arya, R., Kayastha, A.M., Srivastava, K.K., Tripathi, L.M., Saxena, J.K., 2008. Molecular cloning and characterization of *Brugia malayi* hexokinase. Parasitol. Int. 57, 354–361.

Storn, R., Price, K., 1997. Differential evolution – a simple and efficient adaptive scheme for global optimization over continuous spaces. J. Global Opt. 11, 341–359.

Su, J.Y., Sclafani, R.A., 1991. Molecular cloning and expression of the human deoxythymidylate kinase gene in yeast. Nucleic Acids Res. 19, 823–827.

Tamura, K., Peterson, D., Peterson, N., Stecher, G., Nei, M., Kumar, S., 2011. MEGA5: molecular evolutionary genetics analysis using maximum likelihood, evolutionary distance and maximum parsimony methods. Mol. Biol. Evol. 28, 2731–2739.

Thomsen, R., Christensen, M.H., 2006. MolDock: a new technique for high-accuracy molecular docking. J. Med. Chem. 49, 3315–3321.

Van Daele, I., Munier-Lehmann, H., Hendrickx, P.M., Marchal, G., Chavarot, P., Froeyen, M., Qing, L., Martins, J.C., Van Calenbergh, S., 2006. Synthesis and biological evaluation of bicyclic nucleosides as inhibitors of *M. tuberculosis* thymidylate kinase. ChemMedChem 1 (10), 1081–1090.

Vanheusden, V., Munier-Lehmann, H., Froeyen, M., Busson, R., Rozenski, J., Herdewijn, P., Van Calenbergh, S., 2004. Discovery of bicyclic thymidine analogues as selective and high-affinity inhibitors of *Mycobacterium tuberculosis* thymidine monophosphate kinase. J. Med. Chem. 47 (25), 6187–6194.

Vanheusden, V., Munier-Lehmann, H., Froeyen, M., Dugue, L., Heyerick, A., De Keukeleire, D., Pochet, S., Busson, R., Herdewijn, P., Van Calenbergh, S., 2003. 3′-C-branched-chain-substituted nucleosides and nucleotides as potent inhibitors of *Mycobacterium tuberculosis* thymidine monophosphate kinase. J. Med. Chem. 46 (18), 3811–3821.

Vanheusden, V., Munier-Lehmann, H., Pochet, S., Herdewijn, P., Van Calenbergh, S., 2002. Synthesis and evaluation of thymidine-5′-omonophosphate analogues as inhibitors of *Mycobacterium tuberculosis* thymidylate kinase. Bioorg. Med. Chem. Lett. 12 (19), 2695–2698.

Whittingham, J.L., Carrero-Lerida, J., Brannigan, J.A., Ruiz-Perez, L.M., Silva, A.P.G., Fogg, M.J., Wilkinson, A.J., Gilbert, I.H., Wilson, K.S., Gonzalez-Pacanowska, D., 2010. Structural basis for the efficient phosphorylation of AZT-MP (3-azido-3-deoxythymidine monophosphate) and dGMP by *Plasmodium falciparum* type I thymidylate kinase. Biochem. J. 428, 499–509.